Journal of Coordination Chemistry
Publication details, including instructions for authors and subscription information:
http://www.tandfonline.com/loi/gcoo20

Homo and heterodinuclear complexes derived from unsymmetrical macrocyclic ligands with two coordination sites: removal of a pendant arm and migration of copper ion upon cyclization

Hamid Golchoubian [a], Davood Sadeghi Fateh [b], Giuseppe Bruno [c] & Hadi Amiri Rudbari [c]

[a] Department of Chemistry, University of Mazandaran, 47416-95447, Babol-sar, Iran

[b] Department of Chemistry, Mohammad Reza Hariri Science Foundation, 47146-38474, Babol, Iran

[c] Dipartimento di Chimica Inorganica, Università di Messina, Villaggio S Agata, Salita Sperone, 31, 98166 Messina, Italy

Published online: 14 May 2012.

To cite this article: Hamid Golchoubian, Davood Sadeghi Fateh, Giuseppe Bruno & Hadi Amiri Rudbari (2012) Homo and heterodinuclear complexes derived from unsymmetrical macrocyclic ligands with two coordination sites: removal of a pendant arm and migration of copper ion upon cyclization, Journal of Coordination Chemistry, 65:11, 1970-1991, DOI: 10.1080/00958972.2012.687103

To link to this article: http://dx.doi.org/10.1080/00958972.2012.687103

Journal of Coordination Chemistry
Vol. 65, No. 11, 10 June 2012, 1970–1991

Homo and heterodinuclear complexes derived from unsymmetrical macrocyclic ligands with two coordination sites: removal of a pendant arm and migration of copper ion upon cyclization

HAMID GOLCHOUBIAN*†, DAVOOD SADEGHI FATEH‡, GIUSEPPE BRUNO§ and HADI AMIRI RUDBARI§

†Department of Chemistry, University of Mazandaran, 47416-95447, Babol-sar, Iran
‡Department of Chemistry, Mohammad Reza Hariri Science Foundation, 47146-38474, Babol, Iran
§Dipartimento di Chimica Inorganica, Università di Messina, Villaggio S Agata, Salita Sperone, 31, 98166 Messina, Italy

(*Received 18 November 2011; in final form 14 March 2012*)

The dinucleating macrocyclic ligands $(L^{2a})^{2-}$ and $(L^{2b})^{2-}$ were prepared by [1 : 1] cyclic condensation of *N,N′*-dipropionitrile-*N,N′*-ethylene-di(5-methyl-3-formyl-2-hydroxybenzylamine or *N,N′*-dipropionitrile-*N,N′*-ethylene-di(5-bromo-3-formyl-2-hydroxybenzylamine with 1,3-diaminopropane. The ligands include dissimilar $N(amine)_2O_2$ and $N(imine)_2O_2$ coordination sites sharing two phenolic oxygen atoms and containing two propionitrile pendant arms on the amine nitrogen atoms. A series of mono- and dinuclear complexes were synthesized and characterized on the basis of elemental analysis, molar conductance measurement, X-ray crystallography, IR, NMR, and UV-Vis spectroscopies as well as cyclic voltammetric measurements. During the cyclization copper(II) migrates from the $N(amine)_2O_2$ to the $N(imine)_2O_2$ coordination site and one of the propionitrile pendant arms is removed. The heterodinuclear complexes $[ZnL^2Cu(OAc)]^+$ were prepared by a transmetallation reaction. The characterization results showed that the two metal ions are bridged by two phenolic oxygen atoms and an acetate group, providing distorted five-coordinate geometries for both metals.

Keywords: Heterodinuclear complex; Pendant arm ligand; Unsymmetrical compartmental ligand; Macrocyclic ligand; Copper migration; Crystal structure

1. Introduction

Syntheses of macrocyclic unsymmetrical compartmental ligands and their dinuclear complexes have received increasing interest due to unique physicochemical properties associated with metal–metal interactions [1–5], their potential to mimic the active sites of the metalloenzymes [6], their ability to stabilize unusual oxidation states [7], their catalytic properties [8], and also their possibilities for mutual influences of two metal centers on the electronic, magnetic, and electrochemical properties [9]. Among the

*Corresponding author. Email: h.golchobian@umz.ac.ir

ISSN 0095-8972 print/ISSN 1029-0389 online © 2012 Taylor & Francis
http://dx.doi.org/10.1080/00958972.2012.687103

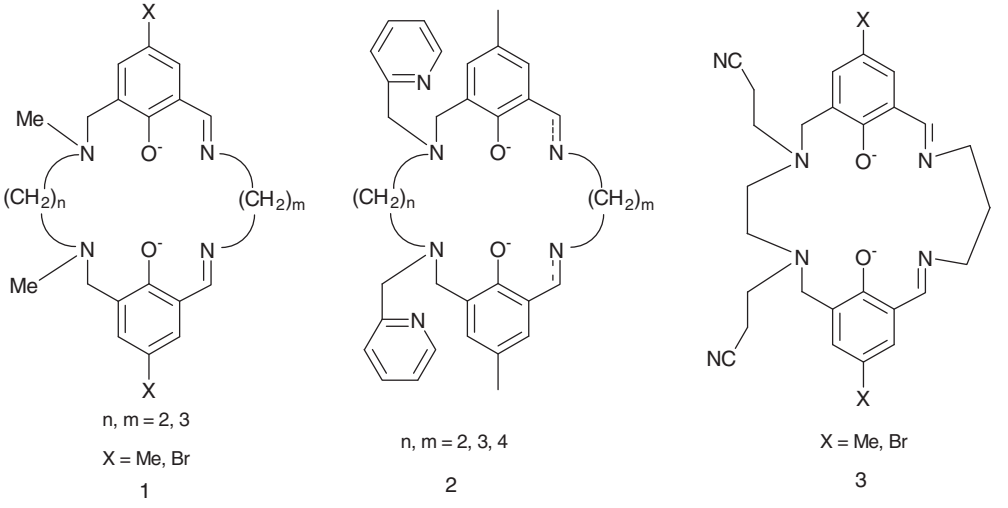

Scheme 1. Phenol-based macrocyclic dicompartmental ligands with pendant arms.

various types of dinucleating ligands, phenol-based two compartmental ligands have been attracted wide attention because of their capabilities to accommodate simultaneously two metal ions in close proximity [10–14]. Many unsymmetrical phenol-based dinucleating ligands with shape and flexibility of the coordination compartment, the nature of donors and their relative position, the number of donors and size of the chelating ring have been developed. Special attention has focused on unsymmetrical compartmental ligands containing two pendant arms as shown in scheme 1 (types 1 and 2) and their metal complexes [15–22]. The pendant arms could have additional potential ligating groups. Okawa and coworkers introduced the unsymmetrical dinucleating ligands type **1** (scheme 1) [23] whose pendant arms were inactive for coordination to metal ions. However, elegant development of unsymmetrical dicompartmental ligand by Bosnich and coworkers [12] made use of ligating picolyl pendant arms attached to the nitrogen donors in one compartment as shown by **2** in scheme 1.

In continuation of our research work on the generation of unsymmetrical ligands with dissimilar compartments [24–29] we report here the synthesis of heterodinuclear complexes with unsymmetrical macrocyclic ligand containing two propionitrile pendant arms, shown as **3** in scheme 1. The idea behind this design was based on results that showed acetonitrile coordinated to Co(II), Ni(II), and Cu(II) [30–32] in macrocyclic complexes type **1** shown in scheme 1.

2. Experimental

2.1. *Materials and measurements*

All chemicals were of analytical grade. Solvents were purified by conventional methods. Elemental analyses were performed by a LECO CHN-600 Elemental Analyzer. Absolute metal percentages were determined by a Varian-spectra A-30/40 atomic

absorption-flame spectrometer. Conductance measurements were made at 25°C with a Jenway 400 conductance meter on 1.00×10^{-3} mol L^{-1} samples in acetonitrile. ^{1}H NMR and ^{13}C NMR spectra were measured with Bruker 500 and 400 DRX Fourier Transform Spectrometers at room temperature. UV-Vis spectra were obtained on a Cicil CE5501 spectrophotometer at room temperature in acetonitrile and solid state. Infrared (IR) spectra were recorded in KBr by a single beam Bruker VECTOR22 FTIR from 400 cm^{-1} to 4000 cm^{-1}. Cyclic voltammograms were recorded using a EG&G Model 263 A interfaced to a PC *via* a GPIB interface from +2 V to −2 V in deaerated CH_3CN with 0.1 mol L^{-1} *n*–Bu_4NPF_6 (TBAHFP) supporting electrolyte and 1.0 mmol L^{-1} sample. Redox potentials were measured using a three-electrode system consisting of a glassy carbon (working), platinum wire (auxiliary), and Ag/Ag^+ (non-aqueous (CH_3CN), reference) electrodes. All samples were dried to constant weight under high vacuum prior to analysis. The compounds 2-hydroxy-3-chloromethyl-5-methylbenzaldehyde and 2-hydroxy-3-chloromethyl-5-bromobenzaldehyde were prepared by standard method [33].

2.2. *Syntheses*

2.2.1. *N,N′*-bis-(2-cyanoethyl)-ethylenediamine. To a deoxygenated aqueous solution (20 mL) of ethylenediamine (13.35 mL, 0.20 mol) acrylonitrile (65.75 mL, 1.00 mol) was added dropwise during 40 min at room temperature. The resultant pale yellow solution was stirred for 30 min and the solvent was then removed under vacuum. The residual of the water was further removed by passing the product through anhydrous $CaCl_2$. The desired diamine formed as a pale yellow liquid (4.9 g, 95%), sufficiently pure for further treatment. IR (ν/cm^{-1}): 2247 (C≡N str.), 2915 and 2847 (C–H str. Aliphatic), 3380 (N–H str.). UV-Vis (nm; ε_{max}) 258 (5360). ^{1}H NMR (400 MHz in D_2O) δ: 2.70 (t, 4 H, $J = 6.8$ Hz, CCH_2CN), 2.76 (s, 4 H, NCH_2CH_2N), 2.93 (t, 4 H, $J = 6.8$ Hz, NCH_2CH_2CN). ^{13}C NMR (100.08 MHz in D_2O) δ: 17.46 (CCH_2CN), 43.95 (NCH_2CH_2CN), 47.13 (NCH_2CH_2N), 120.60 (CH_2CN). Mass spectrum showed the dominant peak at *m*/*e* 114 corresponding to loss of two CN moieties from $C_8H_{14}N_4$.

2.2.2. 1,6-Bis(2-cyanoethyl)-2,5-bis(2-hydroxy-3-formyl-5-methylbenzyl)-2,5-diazahexane, $L^{1a}H_2$. 2-Hydroxy-3-chloromethyl-5-methylbenzaldehyde (0.92 g, 5.0 mmol) was dissolved in 1,3-dioxalane (25 mL) and anhydrous Na_2CO_3 (1.38 g, 13.0 mmol) was added. To the resulting mixture, *N,N′*-bis-(2-cyanoethyl)-ethylenediamine (0.42 g, 2.50 mmol) was added. The reaction mixture, after stirring at 100°C for 6 h, was allowed to cool to room temperature and was then filtered through Celite. Dioxalane was removed in vacuum to give a thick orange-brown oil, which was treated with an aqueous solution of HCl (4 mol L^{-1}) in an ice-bath to reach pH = 1. The yellow suspension was then extracted by CH_2Cl_2 (3 × 20 mL). The aqueous layer was adjusted to pH ≈ 7.0 with aqueous NaOH (40%) and then to pH ≈ 8.4 by the addition of a saturated aqueous solution of $NaHCO_3$. The oily mixture was extracted with CH_2Cl_2 (4 × 10 mL) and the combined organic extracts were dried over Na_2SO_4. Filtration and concentration under reduced pressure gave essentially pure $L^{1a}H_2$ as a pale brown oil, 1.07 g (93%). Although the crude compound can be used in further treatment without any problem it was purified as follows: to an ethanol solution (10 mL) of crude $L^{1a}H_2$ was added

1.4 mL Et_3N (10.0 mmol) and 0.425 g LiCl (10.0 mmol) in absolute ethanol (10 mL) which immediately resulted in a yellow solid. After stirring the reaction mixture for 1 h, the resultant Li_2L^{1a} was collected, washed with ethanol (2×3 mL), Et_2O (2×3 mL), and pentane (2×3 mL) and dried under vacuum. Li_2L^{1a} was obtained as a pale yellow solid. Li_2L^{1a} was converted to pure $L^{1a}H_2$ by dissolving it in dichloromethane (10 mL) with HCl (gas) bubbled slowly through a stirred solution for 5 min. A colorless precipitate formed almost immediately. The solid was separated by filtration. To the colorless precipitate was added an aqueous saturated solution of $NaHCO_3$ (20 mL) and the mixture was then extracted with CH_2Cl_2 (4×10 mL). The resultant organic layers were collected and dried through anhydrous Na_2SO_4. Filtration and concentration under reduced pressure resulted in $L^{1a}H_2$ as a pale yellow oil. In purification almost 70% of the compound was lost. ^{1}H NMR (500.13 MHz in $CDCl_3$) δ: 2.25 (s, 6H, $ArCH_3$), 2.50 (t, $J = 6.4$ Hz, 4H, CH_2–CN), 2.70 (s, 4H, N–CH_2–CH_2–N), 2.84 (t, $J = 6.4$ Hz, 4H, $NCCH_2CH_2$–N), 3.69 (s, 4H, Ar–CH_2–N), 7.27 (s, 2H, Ar–H), 7.34 (s, 2H, Ar–H), 9.91 (s, 2H, Ar–CHO), 11.01 (br, s, 2H, Ar–OH). ^{13}C NMR (125 MHz in $CDCl_3$) δ: 16.2 (CH_2–CN), 20.7 ($ArCH_3$), 44.3 (Ar–CH_2–N), 50.2 ($NCCH_2CH_2$–N), 52.4 (N–CH_2–CH_2–N), 119.3 ($CH_2\underline{C}N$), 121.3 (Ar), 125.7 (Ar), 129.3 (Ar), 131.9 (Ar), 138.7 (Ar), 158.3 (Ar), 195.5 (Ar–$\underline{C}HO$). When one drop of D_2O was added to the ^{1}H NMR sample, the broad signal at 11.01 ppm disappeared. IR (ν/cm^{-1}): 1670 (C=O str.), 2248 (C≡N str.), 2848 (C–H str. aliphatic), 3010 (C–H str. aromatic), 3430 (O–H str.).

2.2.3. 1,6-Bis(2-cyanoethyl)-2,5-bis(2-hydroxy-3-formyl-5-bromobenzyl)-2,5-diazahexane, $L^{1b}H_2$. This compound was prepared (91%) by the method applied for $L^{1a}H_2$ except that 2-hydroxy-3-chloromethyl-5-bromobenzaldehyde was used in place of 2-hydroxy-3-chloromethyl-5-methylbenzaldehyde. ^{1}H NMR (500.13 MHz in $CDCl_3$) δ: 2.57 (t, $J = 6.8$ Hz, 4H, CH_2–CN), 2.81 (s, 4H, N′–CH_2–CH_2–N), 2.91 (t, $J = 6.8$ Hz, 4H, $NCCH_2CH_2$–N), 3.76 (s, 4H, Ar–CH_2–N), 7.69 (s, 2H, Ar–H), 7.70 (s, 2H, Ar–H), 9.98 (s, 2H, Ar–CHO), 11.25 (br, s, 2H, Ar–OH). ^{13}C NMR (125 MHz in $CDCl_3$) δ: 16.5 (CH_2–CN), 50.2 (Ar–CH_2–N), 52.0 ($NCCH_2CH_2$–N), 52.2 (N–CH_2–$\underline{C}H_2$–N), 112.1 (CH_2CN), 119.0 (Ar), 122.7 (Ar), 128.8 (Ar), 134.3 (Ar), 139.8 (Ar), 159.3 (Ar), 194.5 (Ar–CHO). When one drop of D_2O was added to the ^{1}H NMR sample, the broad signal at 11.25 ppm disappeared. IR (ν/cm^{-1}): 1668 (C=O str.), 2248 (C≡N str.), 2831 (C–H str. aliphatic), 3068 (C–H str. aromatic).

2.3. *Metal complexes*

All [ML^1] complexes were prepared by a general procedure described for [$ZnL^{1a}(H_2O)_2$]. All complexes are insoluble in common solvents used and cannot be purified by recrystallization.

[$ZnL^{1a}(H_2O)_2$]: To $L^{1a}H_2$ (1.12 g, 2.1 mmol) and Et_3N (0.88 mL, 4.3 mmol) in ethanol (20 mL) was added $Zn(OAc)_2 \cdot 4H_2O$ (0.44 g, 2.1 mmol) in methanol (10 mL). The initial pale yellow solution turned yellow and a yellow precipitate formed almost immediately. The reaction mixture was stirred for 6 h. The solid was collected with suction filtration and washed with methanol (2×10 mL), Et_2O (2×10 mL) and hexane (2×10 mL) and dried in vacuum. [$ZnL^{1a}(H_2O)_2$] was obtained as a yellow solid (0.60 g, 51%). Selected IR data (ν/cm^{-1} using KBr): 3468 (m, O–H str.), 2931 and 2848 (w, C–H str.), 2249

(w, C≡N str.), 1659 (s, C=O str.), 1457 (s, C=C str. aromatic). Anal. Calcd for $C_{26}H_{28}N_4O_4Zn \cdot 2H_2O$ ($M_w = 561.94\,g\,mol^{-1}$) (%): C, 55.57; H, 5.74; N, 9.97; Zn, 11.63. Found (%): C, 54.90; H, 6.18; N, 9.64; Zn, 11.31.

$[ZnL^{1b}(H_2O)_2]$: This complex formed as a yellow solid with yield of 52%. Selected IR data (ν/cm^{-1} using KBr): 3435 (m, O–H str.), 2926 and 2853 (m, C–H str.), 2248 (m, C≡N str.), 1656 (s, C=O str.), 1439 (s, C=C str. aromatic). Anal. Calcd for $C_{24}H_{22}N_4O_4ZnBr_2 \cdot 2H_2O$ ($M_w = 691.68\,g\,mol^{-1}$) (%): C, 41.68; H, 3.79; N, 8.10; Zn, 9.45. Found (%): C, 42.18; H, 4.07; N, 8.64; Zn, 9.27.

$[CuL^{1a}] \cdot 2H_2O$ was obtained as a blue solid (55%). Selected IR data (ν/cm^{-1} using KBr): 3431 (m, O–H str.), 2925 and 2840 (m, C–H str.), 2248 (m, C≡N str.), 1651 (s, C=O str.), 1614 (m, C=C str. aromatic), 1461, 1269. Anal. Calcd for $C_{26}H_{28}N_4O_4Cu \cdot 2H_2O$ ($M_w = 560.11\,g\,mol^{-1}$) (%): C, 55.75; H, 5.76; N, 10.00; Zn, 11.35. Found (%): C, 56.20; H, 6.12; N, 9.49; Zn, 11.17.

$[CuL^{1b}] \cdot 2H_2O$ was obtained as a blue solid with yield of 53%. Selected IR data (ν/cm^{-1} using KBr): 3422 (m, O–H str.), 2931 and 2847 (m, C–H str.), 2247 (m, C≡N str.), 1660 (s, C=O str.), 1426 (s, C=C str. aromatic). Anal. Calcd for $C_{24}H_{22}N_4O_4CuBr_2 \cdot 2H_2O$ ($M_w = 689.85\,g\,mol^{-1}$) (%): C, 41.79; H, 3.80; N, 8.12; Zn, 9.21. Found (%): C, 42.23; H, 4.39; N, 7.69; Zn, 9.00.

Demetallation of $[CuL^{1a}] \cdot 2H_2O$: $[CuL^{1a}] \cdot 2H_2O$ (0.2 g, 0.36 mmol) was suspended in 100 mL of chloroform and H_2S gas was bubbled slowly through it and stirred for 30 min. The resulting black suspension of CuS was removed by filtration through Celite. The chloroform was distilled from the solution under reduced pressure. The yellow residue was dissolved in methanol (15 mL), sonicated, filtered through Celite, and concentrated under reduced pressure to give the pure free ligand $L^{1a}H_2$ as a yellow oil (14 g, 84%). The observed ^1H NMR and ^{13}C NMR spectra were identical with those described for $L^{1a}H_2$.

$[(H^+)L^{3a}Cu]PF_6$: To stirred suspension of $[CuL^{1a}(H_2O)_2]$ (0.29 g, 0.63 mmol) in ethanol (40 mL) was added dropwise over 45 min a solution of 1,3-diaminopropane (0.055 mL, 0.63 mmol) and acetic acid (0.072 mL, 1.25 mmol) in ethanol (20 mL). After the addition was complete, all starting materials were dissolved. The resulting blue solution was then stirred for 3 h at room temperature. A dark blue solid precipitated almost immediately after addition of a filtered saturated solution of NH_4PF_6 in ethanol. The solid was collected and washed with ethanol (2×10 mL), Et_2O (2×5 mL) and hexane (2×5 mL). The crude compound was recrystallized by diffusion of diethyl ether into CH_3CN solution, yielding a blue solid (0.22 g, 53%). Crystals suitable for X-ray crystal structure determination were grown by vapor diffusion of ethanol into a $CH_3CN : C_2H_5OH$ solution of the complex. Selected IR data (ν/cm^{-1} using KBr): 3247 (m, N–H str.), 2923 and 2859 (m, C–H str.), 2247 (m, C≡N str.), 1621 (s, C=N str.), 1447 (s, C=C Ar), 842 and 558 (s, PF_6 str.). Anal. Calcd for $C_{26}H_{31}N_5O_2CuPF_6$ ($M_w = 654.07\,g\,mol^{-1}$) (%): C, 47.74; H, 4.78; N, 10.71; Cu, 9.72. Found (%): C, 47.41; H, 5.12; N, 10.52, Cu; 10.01.

$[(H^+)L^{3b}Cu]PF_6$ was prepared by the same procedure described above except that $[CuL^{1b}(H_2O)_2]$ was used in place of $[CuL^{1a}(H_2O)_2]$. The product was obtained as a blue solid with yield of 50%. Selected IR data (ν/cm^{-1} using KBr): 3237 (m, N–H str.), 3054, 2927 and 2852 (m, C–H str.), 2248 (m, C≡N str.), 1614 (s, C=N str.), 1451 (s, C=C Ar.), 843 and 558 (s, PF_6 str.). Anal. Calcd for $C_{24}H_{25}N_5O_2CuBr_2PF_6$ ($M_w = 770.81\,g\,mol^{-1}$) (%): C, 36.78; H, 3.21; N, 8.93; Cu, 8.11. Found (%): C, 37.05; H, 3.51; N, 8.62; Cu, 8.14.

$[ZnL^{2a}Zn(OAc)]PF_6$: $[ZnL^{1a}(H_2O)_2]$ (0.30 g, 0.63 mmol) was suspended in ethanol (30 mL) and then a solution of 1,3-diaminopropane (0.055 mL, 0.63 mmol) and acetic acid (0.072 mL, 1.25 mmol) in ethanol (20 mL) was added dropwise over 30 min. After all starting materials dissolved, a solution of $Zn(OAc)_2 \cdot 4H_2O$ (0.138 g, 0.63 mmol) in ethanol (10 mL) was added. The reaction mixture was stirred for 1 h and then a saturated solution of NH_4PF_6 in ethanol was added. The resulting yellow solid was collected and washed with ethanol (2×10 mL), ether (2×10 mL) and pentane (2×10 mL). The crude compound was recrystallized by diffusion of diethyl ether into CH_3CN solution, yielding yellow-orange crystals (0.24 g, 46%). Crystals suitable for X-ray crystal structure determination were grown by vapor diffusion of ethanol into a CH_3CN: ethanol solution of the complex. Anal. Calcd for $C_{31}H_{37}N_6O_4PF_6Zn_2$ ($M_w = 833.40\ g\ mol^{-1}$) (%): C, 44.68; H, 4.47; N, 10.08; Zn, 15.69. Found: C, 44.48; H, 4.36; N, 9.94; Zn, 15.63. Selected IR data (ν/cm^{-1} using KBr): 3053 (w, C–H str. aromatic), 2925, 2859, and 2746 (m, C–H str.), 2249 (m, C≡N str.), 1653 (s, C=N str.), 1571, and 1463 (s, C=O str. OAc), 1442 (m, C=C str. aromatic), 1327 (s, Ph–O str.) 843, and 558 (s, PF_6 str.). ^1H NMR (500 MHz, CD_3CN), 1.96 (s, 3H, CH_3–COO), 2.21 (m, 2H), 2.28 (s, 6H, $ArCH_3$), 2.75 (m, 4H), 2.97 (m, 2H), 3.15 (m, 4H), 3.28, (m, 2H), 3.66 (s, 1H), 3.68 (s, 1H), 3.99 (m, 4H), 4.31 (s, 1H), 4.33 (s, 1H), 7.21 (s, 2H, Ar), 7.25 (s, 2H, Ar), 8.32 (s, 2H, ArCH=N). ^{13}C NMR (125 MHz in CD_3CN) δ: 10.06, 14.79, 19.15, 28.97, 46.34, 50.42, 55.64, 61.89, 118.17, 118.61, 123.12, 126.02, 136.67, 137.29, 162.78, 166.19, 170.96.

$[ZnL^{2b}Zn(OAc)]PF_6$ was prepared with the same procedure as $[ZnL^{2a}Zn(OAc)]PF_6$ except that $[ZnL^{1b}(H_2O)_2]$ was used instead of $[ZnL^{1a}(H_2O)_2]$ giving a yellow solid with yield of 53%. Anal. Calcd for $C_{29}H_{31}N_6O_4PF_6Br_2Zn_2$ ($M_w = 963.14\ g\ mol^{-1}$) (%): C, 36.17; H, 3.24; N, 8.73; Zn, 13.58. Found: C, 36.51; H, 3.02; N, 9.02; Zn, 13.48. Selected IR data (ν/cm^{-1} using KBr): 3033 (w, C–H str. aromatic), 2931, 2850 and 2749 (m, C–H str.), 2248 (m, C≡N str.), 1655 (s, C=N str.), 1573 and 1460 (s, C=O str. OAc), 1446 (m, C=C str. aromatic), 1324 (s, Ph–O str.), 844 and 558 (s, PF_6 str.). ^1H NMR (400 MHz, CD_3CN), 1.83 (s, 3H, CH_3COO), 2.75 (m, 4H), 3.02 (m, 3H,), 3.16 (m, 4H), 3.28 (m, 2H), 3.40 (s, 1H), 3.73, (s, 1H), 3.97 (m, 5H), 4.34 (s, 1H), 4.38 (s, 1H), 7.58 (d, AB system, 2H, Ar), 7.60 (s, AB system, 2H, Ar), 8.32 (s, 2H, ArCH=N). ^{13}C NMR (100 MHz in $CDCl_3$) δ: 10.14, 22.76, 28.62, 46.39, 50.39, 55.13, 61.99, 107.06, 117.33, 118.13, 120.59, 125.82, 138.38, 138.63, 164.06, 169.86.

All heterodinuclear complexes were prepared by a general procedure described for $[ZnL^{2a}Cu(OAc)]PF_6$.

$[ZnL^{2a}Cu(OAc)]PF_6 \cdot CH_3CN$: To a solution of $[ZnL^{2a}Zn(OAc)]PF_6$ (178 mg, 2.0 mmol) in CH_3CN (10 mL) was added a solution of $Cu(OAc)_2 \cdot H_2O$ (48 mg, 2.4 mmol) in ethanol (10 mL). The brown reaction mixture was stirred for 1 h. A saturated solution of NH_4PF_6 in ethanol was added to the resultant solution. The solution was partially concentrated at room temperature to reduce CH_3CN content; ethanol was then added in portions of (2×10 mL) and the solution was allowed to stand overnight. The solid was collected and washed with ethanol (2×10 mL), ether (2×10 mL), and pentane (2×10 mL). The crude compound was recrystallized by diffusion of diethyl ether into CH_3CN solution, which yielded blue crystals (0.11 g, 63%). Crystals suitable for X-ray crystal structure determination were grown by vapor diffusion of ethanol into a $CH_3CN : C_2H_5OH$ solution of the complex. Selected IR data (ν/cm^{-1} using KBr): 2925 and 2839 (m, C–H str.), 2248 (m, C≡N str.), 1623 (s, C=N str.), 1572 and 1403

(s, C=O str. OAc), 1440 (s, C=C str. aromatic), 1329 (s, Ph–O str.), 844 and 558 (s, PF_6 str.). Anal. Calcd for $C_{33}H_{40}N_7O_4PF_6ZnCu$ ($M_w = 872.62\,g\,mol^{-1}$) (%): C, 45.42; H, 4.62; N, 11.24; Zn, 7.49; Cu, 7.28. Found: C, 45.01; H, 4.73; N, 11.45; Zn, 7.60; Cu, 7.43.

$[ZnL^{2b}Cu(OAc)]PF_6$ was obtained as a blue solid with yield of 65%. Selected IR data (ν/cm^{-1} using KBr): 2926 (m, C–H str.), 2251 (m, C≡N str.), 1623 (s, C=N str.), 1573 and 1444 (s, C=O str. OAc), 1399 (m, C=C str. aromatic), 1304 (s), 845 and 559 (s, PF_6 str.). $C_{29}H_{31}N_6O_4PF_6Br_2ZnCu$ ($M_w = 961.30\,g\,mol^{-1}$) (%): C, 36.23; H, 3.25; N, 8.74; Zn, 6.80; Cu, 6.61. Found: C, 36.58; H, 2.99; N, 8.91; Zn, 6.62; Cu, 6.53.

$[ZnL^{3a}Cu(OAc)]PF_6$ was obtained as a blue solid with yield of 75%. Selected IR data (ν/cm^{-1} using KBr): 3282 (m, N–H str.), 2935 (m, C–H str.), 2254 (m, C≡N str.), 1623 (s, C=N str.), 1588 and 1567 (m, C=O str. OAc), 1447 (s, OAc), 1400 (s, C=C str.), 1332 (m, Ph–O str.), 1305 (s), 844 and 558 (s, PF_6 str.). $C_{28}H_{32}N_5O_4PF_6ZnCu$ ($M_w = 776.48\,g\,mol^{-1}$) (%): C, 43.31; H, 4.15; N, 9.02; Zn, 8.42; Cu, 8.18. Found (%): C, 43.66; H, 3.87; N, 8.84; Zn, 8.25; Cu, 8.00.

$[ZnL^{3b}Cu(OAc)]PF_6$ was obtained as a blue solid with yield of 77%. Selected IR data (ν/cm^{-1} using KBr): 3282 (m, N–H str.), 2930 and 2848 (m, C–H str.), 2254 (m, C≡N str.), 1627 (s, C=N str.), 1577 and 1440 (s, C=O str. OAc), 1401 (s, C=C str.), 1334 (s, Ph–O str.), 844 and 558 (PF_6 str.). $C_{26}H_{26}N_5O_4Br_2PF_6ZnCu$ ($M_w = 906.22\,g\,mol^{-1}$) (%): C, 34.46; H, 2.89; N, 7.73; Zn, 7.21; Cu, 7.01. Found: C, 34.13; H, 3.09; N, 7.62; Zn, 7.48, Cu, 7.33.

$[CuL^{3a}Cu(OAc)]PF_6 \cdot 1.5\ H_2O$ was obtained as a blue solid with yield of 78%. Selected IR data (ν/cm^{-1} using KBr): 3278 (m, N–H str.), 2925 and 2852 (m, C–H str.), 2253 (m, C≡N str.), 1623 (s, C=N str.), 1575 (s, C=O str. OAc), 1448 (s, C=C str.), 1334 (s, Ph–O str.), 844 and 558 (s, PF_6 str.). $C_{28}H_{37}Cu_2F_6N_5O_{5.5}P$ ($M_w = 815.70\,g\,mol^{-1}$) (%): C, 42.70; H, 4.57; N, 8.50; Cu, 15.58. Found: C, 43.04; H, 4.25; N, 8.18; Cu, 15.44.

2.4. *X-ray crystallographic study*

The X-ray measurement of $[(H^+)L^{3a}Cu]PF_6$, $[ZnL^{2a}Zn(OAc)]PF_6$, $[ZnL^{2a}Cu(OAc)]PF_6$, and $[CuL^{3a}Cu(OAc)]PF_6$ were made on a Bruker-Nonius X8 ApexII diffractometer equipped with a CCD area detector by using graphite-monochromated Mo-Kα radiation ($\lambda = 0.71073$ Å) generated from a sealed tube source. Data were collected and reduced by SMART and SAINT software [34] in the Bruker packages. The structures were solved by direct methods [35] and then developed by least-squares refinement on F^2 [36, 37]. The complete conditions of data collection and structure are given in table 1.

All hydrogen atoms were refined in isotropic approximation in riding model with U_{iso}(H) parameters equal to $1.2U_{eq}$(Ci), for methyl groups equal to $1.5U_{eq}$(Cii), where U(Ci) and U(Cii) are, respectively, the equivalent thermal parameters of the carbon atoms to which corresponding hydrogen atoms are bonded. Refinement of F^2 was against all reflections. The weighted R-factor wR and goodness-of-fit S are based on F^2, conventional R-factors are based on F, with F set to zero for negative F^2. The threshold expression of $F^2 > 2\sigma(F^2)$ is used only for calculating R-factors(gt) etc., and is not relevant to the choice of reflections for refinement.

Table 1. Crystallographic data.

	$[(H^+)L^{3a}Cu]PF_6$	$[ZnL^{2a}Zn(OAc)]PF_6$	$[ZnL^{2a}Cu(OAc)]PF_6 \cdot CH_3CN$	$[CuL^{3a}Cu(OAc)]PF_6 \cdot 1.5H_2O$
Empirical formula	$C_{26}H_{32}CuF_6N_5O_2P$	$C_{58}H_{78}C_{l0}F_{12}N_{12}O_{10}P_2Zn_4$	$C_{33}H_{40}CuF_6N_7O_4PZn$	$C_{28}H_{37}Cu_2F_6N_5O_{5\cdot5}P$
Formula weight	655.08	1654.74	872.60	803.68
Temperature (K)	150(1)	293(2)	150(1)	150(1)
Wavelength (Å)	0.71073	0.71073	0.71073	0.71073
Crystal system	Triclinic	Triclinic	Monoclinic	Triclinic
Space group	$P(-1)$	$P(-1)$	$P\ 21/c$	$P(-1)$
Unit cell dimensions (Å, °)				
a	8.9571(3)	12.935	12.8672(5)	8.5595(2)
b	12.1202(7)	13.182	20.6876(7)	11.1377(3)
c	13.5917(6)	24.948	15.2325(5)	18.5075(6)
α	90.091(2)	82.03	90	73.931(1)
β	88.664(3)	81.13	112.325(1)	87.148(1)
γ	73.341(3)	61.14	90	89.175(1)
Volume (Å^3), Z	1413.17(11), 2	3670.9(1), 2	3750.8(2), 4	1693.34(8), 2
Calculated density (g cm^{-3})	1.582	1.436	1.545	1.576
Absorption coefficient (mm^{-1})	0.903	1.429	1.326	1.382
Crystal size (mm^3)	$0.16 \times 0.08 \times 0.0$	$0.18 \times 0.24 \times 0.20$	$0.35 \times 0.20 \times 0.08$	$0.28 \times 0.12 \times 0.04$
Independent reflection	6372 [R(int) = 0.0604]	17,878 [R(int) = 0.0259]	7378 [R(int) = 0.0307]	6560 [R(int)= 0.0439]
Data/restraints/parameters	6372/36/403	17,878/0/956	7378/16/474	6560/8/467
Goodness-of-fit on F^2	1.032	1.097	1.020	1.067
Final R indices [$I > 2\sigma(I)$]	$R_1 = 0.0586$, $wR_2 = 0.1253$	$R_1 = 0.0447$, $wR_2 = 0.1253$	$R_1 = 0.0599$, $wR_2 = 0.1413$	$R_1 = 0.0622$, $wR_2 = 0.1748$
R indices (all data)	$R_1 = 0.1182$, $wR_2 = 0.1536$	$R_1 = 0.0560$, $wR_2 = 0.1340$	$R_1 = 0.0958$, $wR_2 = 0.1683$	$R_1 = 0.0882$, $wR_2 = 0.1923$
Largest difference peak and hole (e Å^{-3})	0.841 and −0.658	1.010 and −0.809	1.249 and −0.725	1.952 and −0.738

$w = 1/[\sigma^2(F_o^2) + (0.0001\,P)^2 + 15.8676\,P]$.
$P = (F_o^2 + 2F_c^2)/3$.
$S = \sum[w(F_o^2 - F_c^2)^2/(N_{obs} - N_{param})]^{1/2}$.

3. Results and discussion

3.1. *Synthesis*

The amine of the precursor dialdehyde acyclic ligand L^1H_2 was prepared by reactions depicted in scheme 2. Condensation of one part of ethylenediamine and two parts of acrylonitrile resulted in the desired diamine compound with 95% yield (scheme 2, reaction 1). Subsequently, introduction of two molecules of 4-substituted-2-formyl-6-chloromethylphenol and a diamine molecule in dioxalan at reflux resulted in the formation of the precursor dialdehyde L^1H_2 as a viscous oil (scheme 2, reaction 2). The crude compound was purified through replacement of protons of the phenols by lithium ions that resulted in solid Li_2L^1. Subsequent acidification of the solids yields purified L^1H_2 (scheme 2, reaction 3); 70% of yield is lost in the purification process. Acidification was done here to recover the organic ligand; however, this is not always necessary because we have also been successful in directly using Li_2L^1 in preparations of the mononuclear complexes.

Mononuclear $Zn^{II}L^1$ and $Cu^{II}L^1$ were readily obtained as solids by allowing L^1H_2 (or Li_2L^1) to react with the metal acetate and triethylamine in ethanol (scheme 2, reaction 4). The metal in the acyclic $M^{II}L^1$ complex can bind at either the $N(amine)_2O_2$ or at the O_4 coordination site of the ligand. The IR spectrum and the solid state visible spectral data (discussed later) indicate that the metal ion resides in the $N(amine)_2O_2$ coordination site. The $M^{II}L^{1a}$ and $M^{II}L^{1b}$ complexes were nearly insoluble in all solvents investigated, hindering characterization and establishment of the purity of these compounds.

Having the structure of $M^{II}L^1$ as shown in scheme 2, which fixes the orientation of the two aldehydes, it was expected that $M^{II}L^1$ would condense with 1,3-diaminopropane to give the desired macrocyclic complex. This proves to be the case but the results were dependent on the nature of M(II). Thus addition of an equivalent of 1,3-diaminopropane to ZnL^1 under acid catalysis yielded the unexpected dinuclear macrocyclic product $[ZnL^2Zn(OAc)]^+$ instead of mononuclear compound (scheme 2, reaction 6) with yield of 35%. All attempts to obtain mononuclear $[ZnL^2(H^+)_2]^{2+}$ by varying the reaction conditions have failed. However, the analogous ligand system with two pyridine pendant arms in place of the propionitrile generates the macrocyclic mononuclear complex $[ZnL^2(H^+)_2]^{2+}$ [10–13]. As a result, to improve the yield of the reaction an extra equivalent of $Zn(OAc)_2$ was used that resulted an increase in the yield of the reaction (50%). The mononuclear Cu(II) complex, $[(H^+)L^3Cu]^+$, was prepared by a rather unusual route involving migration of copper from $N(amine)_2O_2$ site to the $N(imine)_2O_2$ site along with bond rupture of a propionitrile pendant arm and formation of a secondary amine (scheme 2, reaction 7). The characterization results confirm the presence of a proton in the vacant $N(amine)_2O_2$ site. Removal of the propionitrile pendant arm in introduction of $Cu(OAc)_2$ to the free ligand L^1H_2 was ruled out by lack of the N–H vibration in the IR spectra of CuL^{1a} and CuL^{1b} complexes and also by similarity of their IR spectra with those of the ZnL^{1a} and ZnL^{1b} complexes. This was further confirmed by demetallation of the acyclic copper(II) complex, $Cu^{II}L^{1a}$ by H_2S gas (scheme 2, reaction 5). Characterization of the isolated ligand by NMR spectroscopy revealed both propionitrile pendant arms in the demetallated ligand. The driving force in the migration of Cu(II) may be related to the nature of the donors of the compartments. Cu(II) migrates to occupy the relatively rigid $N(imine)_2O_2$

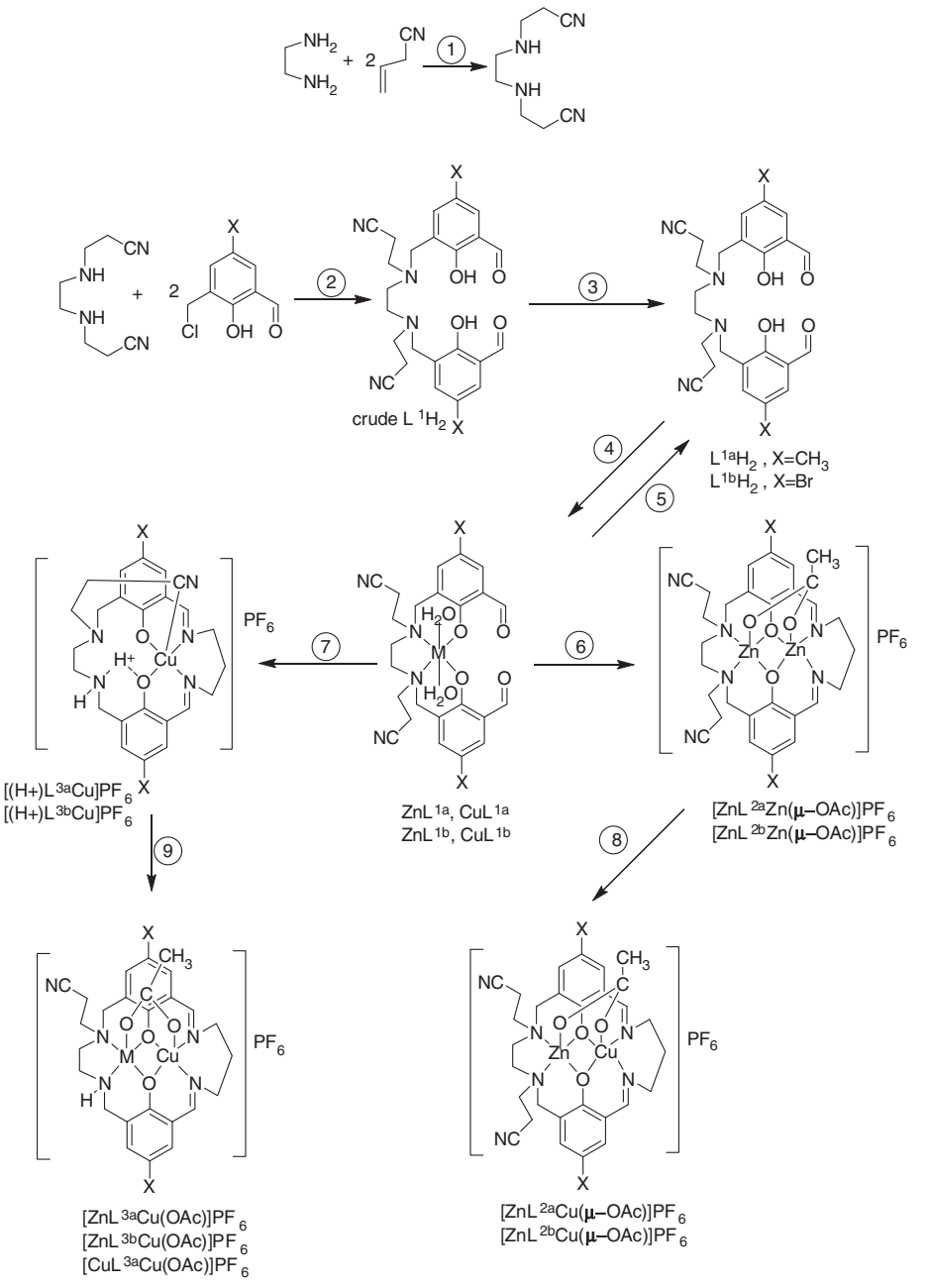

Scheme 2. Synthetic transformations. The following reagents/solvents were used. Reaction 1: ambient conditions in aqueous solution. Reaction 2: reflux in dioxalane in the presence of anhydrous Na_2CO_3. Reaction 3: (a) LiCl (2 equiv.), Et_3N (2 equiv), in methanol and ethanol; (b) HCl (gas) in dichloromethane, followed by the addition of $NaHCO_3$ (aq), extraction of the ligand in dichloromethane. Reaction 4: $Zn(OAc)_2 \cdot 4H_2O$ or $Cu(OAc)_2 \cdot H_2O$, triethylamine (2 equiv), methanol, and ethanol. Reaction 5: [CuL^{1a}], H_2S gas, $CHCl_3$. Reaction 6: [ZnL^1], 1,3-diaminopropane, acetic acid (2 equiv), and $Zn(OAc)_2$ (an equiv) in ethanol followed by the addition of NH_4PF_6 (satur.). Reaction 7: [CuL^1], 1,3-diaminopropane, acetic acid (2 equiv) in ethanol followed by the addition of NH_4PF_6 (satur.). Reaction 8: [$ZnL^2Zn(OAc)$]PF_6, $Cu(OAc)_2 \cdot H_2O$, in acetonitrile/ethanol followed by the addition of NH_4PF_6 (satur.). Reaction 9: [$(H^+)L^3Cu$]PF_6, $Zn(OAc)_2 \cdot 4H_2O$, or $Cu(OAc)_2 \cdot H_2O$, triethylamine (1 equiv) in acetonitrile/ethanol followed by the addition of NH_4PF_6 (satur.).

coordination site, which provides the preferred square-planar environment, but Zn(II) resides in the more flexible $N(amine)_2O_2$ site [30]. Migration of copper ion from aminic to iminic site in the formation of the mononuclear macrocyclic complex type 1 in scheme 1 was reported previously by Bouyagui *et al*. [38]. However, their procedure involved utilization of macro-acyclic CuL complex, diamine link, and $Er(NO_3)_2$ in which Er(II) was not engaged in coordination with the macrocyclic complex.

The heterodinuclear complexes incorporating copper(II) in the $N(imine)_2O_2$ and zinc(II) ion in the $N(amine)_2O_2$ coordination sites were prepared through two different routes. Mononuclear $[(H^+)L^3Cu]^+$ is an ideal precursor for mild synthesis of $[ZnL^3Cu(OAc)]^+$. The reaction depicted in equation (1) can be driven to the right by addition of an exceptionally mild base since incorporation of the second metal depends on the fast removal of the cavity protons. Under such circumstances coordination of the second metal would be much faster than site scrambling of the metals [10]. Starting from the mononuclear complexes, the heterodinuclear complexes $[ZnL^{3a}Cu(OAc)]PF_6$ and $[ZnL^{3b}Cu(OAc)]PF_6$ were prepared by the method illustrated in scheme 2 (reaction 9). In the second route, $[ZnL^{2a}Cu(OAc)]^+$ and $[ZnL^{2b}Cu(OAc)]^+$ were synthesized by transmetallation. The reaction was carried out by the addition of $Cu(OAc)_2$ to dinuclear $[ZnL^2Zn(OAc)]^+$ at room temperature (scheme 2, reaction 8) with moderate yield. It was found that the optimum mole ratio of the reactants between $[ZnL^2Zn(OAc)]^+$ and Cu(OAc) is 1 : 1.2.

$$\left[(H^+)L^3Cu\right]^+ + Zn(OAc)_2 \rightarrow \left[ZnL^3Cu(OAc)\right]^+ + HOAc. \quad (1)$$

Okawa and co-workers carried out extensive work on coordination-position isomers of heterodinuclear complexes using the macrocyclic ligands as shown by 1 in scheme 1 [39]. Site specificity of metal ions at the $N(amine)_2O_2$ site or $N(imine)_2O_2$ site of Cu(II)–Zn(II) complexes depend on the synthetic procedure and the nature of the counter-anion. For instance, the reaction of macrocyclic mononuclear Cu(II) complexes with $ZnCl_2$ provided the heterodinuclear complexes with Cu(II) residing in the $N(imine)_2O_2$ compartment and the Zn(II) occupied the $N(amine)_2O_2$ site. Transmetallation of Pb(II) in Pb(II)–Cu(II) for a Zn(II) ion afforded Zn(II)–Cu(II) perchlorate complexes in which Cu(II) migrates from the $N(imine)_2O_2$ site to the $N(amine)_2O_2$ site; migration is kinetically controlled by geometrical characteristic of the macrocyclic ligand.

3.2. *Physical characterization*

3.2.1. Electronic absorption spectra. The electronic absorption spectra of the mono- and dinuclear complexes were recorded in acetonitrile solutions from 200 nm to 900 nm, including d–d transition and some metal-ligand charge transfer bands. In the spectra, the charge transfer bands overlap with d–d bands of Cu(II). A d–d band is observed in the solid state spectrum at 665 nm for $[CuL^{1a}]$ and 660 nm for $[CuL^{1b}]$, indicative of Cu(II) in the $N(amine)_2O_2$ coordination site [23]. Cu(II) in a $N(amine)_2O_2$ coordination site with square-planar geometry shows a d–d transition around 645–670 nm [40, 41]. A d–d transition is observed for $[(H^+)L^{3a}Cu]^+$ and $[(H^+)L^{3b}Cu]^+$ at 584–581 nm. The d–d band of $[(H^+)L^3Cu]^+$ is comparable to those of *N,N′*-1,3-trimethylenesalicylideneaminato copper(II) (602 in nujol mull) [42] and copper(II) complexes with similar structures (600 nm in DMF) [23]. These results support that copper(II) shifts from $N(amine)_2O_2$

Table 2. Electronic absorption maxima (nm) and intensities (mol L^{-1} cm^{-1}) of the charge transfer and d–d transitions for Cu(II) complexes in CH_3CN.

Compound	π–π^*	d–d
$[CuL^{1a}]$	285	665
$[CuL^{1b}]$	281	660
$[(H^+)L^{3a}Cu]PF_6$	371 (9430)	584 (190), 690 sh (58)
$[(H^+)L^{3b}Cu]PF_6$	351 (9840)	581 (214), 690 sh (85)
$[ZnL^{2a}Cu(OAc)]PF_6$	351 (7670)	674 (125)
$[ZnL^{2b}Cu(OAc)]PF_6$	352 (6790)	670 (140)
$[ZnL^{3a}Cu(OAc)]PF_6$	360 (7340)	678 (130)
$[ZnL^{3b}Cu(OAc)]PF_6$	350 (6680)	673 (138)
$[CuL^{3a}Cu(OAc)]PF_6$	352 (8250)	676 (142)

Electronic absorption spectra for $[CuL^{1a}]$ and $[CuL^{1b}]$ were taken in solid state.

coordination site to the $N(imine)_2O_2$ coordination site upon cyclization of $[CuL^1]$ and the $N(amine)_2O_2$ coordination site is free from coordination (see scheme 2). This is proved by X-ray crystallography for $[(H^+)L^{3a}Cu]PF_6$ as described below. The d–d band in $[ZnL^2Cu(OAc)]PF_6$ and $[ZnL^3Cu(OAc)]PF_6$ moves to a longer wavelength (674 and 678 nm, respectively) relative to the corresponding mononuclear copper(II) complexes due to square-pyramidal geometry about copper(II) [30]. The intense band at 360 nm in macrocyclic complexes is assigned to the π–π^* transition associated with azomethine linkages [39]. Table 2 lists the positions and intensities of the phenolate charge-transfer and the d–d bands observed in the spectra of the complexes.

3.2.2. IR spectra. The IR spectrum of *N*,*N*′-bis-(2-cyanoethyl)-ethylenediamine shows a strong $\nu(C{\equiv}N)$ at 2247 cm^{-1} and a sharp band with medium intensity at 3380 cm^{-1} due to N–H vibration. The former band appears with minor change in the IR spectra of $L^{1a}H_2$ and $L^{1b}H_2$ but the latter is not present in the free ligands. IR spectra of all mononuclear dialdehyde $[ML^{1a}]$ and $[ML^{1b}]$ complexes are nearly identical irrespective of the metal ions used and $\nu(C{\equiv}N)$ appears in the same position as the free ligands indicating that nitrogen of the propionitrile pendant arms are not involved in coordination. The $[ZnL^1]$ and $[CuL^1]$ complexes show an intense $\nu(C{=}O)$ of the formyl at 1660 cm^{-1}. The main spectral differences between the acyclic dialdehyde and the macrocyclic diimine complexes in the spectra are the emergence of two sharp bands at 840 and 560 cm^{-1}, attributed to the anti-symmetric stretching and anti-symmetric bending vibrations of PF_6^-, respectively [43, 44]. Strong evidence that the aldehydes had been completely converted into imine groups was provided by the disappearance of the aldehyde C=O stretch and the appearance of a strong band at 1640 cm^{-1} assigned to C=N stretch [45, 46]. Emergence of a band near 3240 cm^{-1}, attributed to N–H stretch of the quaternized amine, for $[(H^+)L^3Cu]^+$ and also the presence of the $\nu(C{\equiv}N)$ at 2247 cm^{-1} indicate dissociation of an aminonitrile pendant arm. Strong evidence for coordination of the second metal in the $N(imine)_2O_2$ or $N(imine)_2O_2$ coordination site is the appearance of the phenolic stretch at 1320–1334 cm^{-1}, which is absent in this region in the mononuclear complexes [47].

IR spectra of the dinuclear complexes show anti-symmetric and symmetric $\nu(COO)$ vibrations of acetate at 1572 and 1462 cm^{-1}, respectively. The small separation between the two vibration modes (<150 cm^{-1}) indicates bridging acetate in the complex [48].

Table 3. Molar conductivities of the complexes in acetonitrile.[a]

Compound	Λ_m of the complexes ($\Omega^{-1}cm^2 mol^{-1}$, at 25°C)
$[(H^+)L^{3a}Cu]PF_6$	123
$[(H^+)L^{3b}Cu]PF_6$	134
$[ZnL^{2a}Zn(OAc)]PF_6$	146
$[ZnL^{2b}Zn(OAc)]PF_6$	155
$[ZnL^{2a}Cu(OAc)]PF_6$	119
$[ZnL^{2b}Cu(OAc)]PF_6$	151
$[ZnL^{3a}Cu(OAc)]PF_6$	129
$[ZnL^{3b}Cu(OAc)]PF_6$	145
$[CuL^{3a}Cu(OAc)]PF_6$	137
1 : 1 electrolytes	120–160
1 : 2 electrolytes	220–300

[a]Concentration: *ca* 1.0×10^{-3} mol L^{-1}.

The $\nu_{as}(COO^-)$ and $\nu_s(COO^-)$ in the heterodinuclear complexes at 1570 cm^{-1} and 1440 cm^{-1}, respectively, confirm bidentate acetate.

3.2.3. Conductometric data. Molar conductance data, Λ_m, of all of the ionic complexes determined in acetonitrile at 25°C are presented in table 3. The values are accurate to $\pm 5\,\Omega^{-1}\,cm^2\,mol^{-1}$. The standard values of 1 : 1 and 1 : 2 electrolytes in acetonitrile are shown in the same table [43]. The results are in agreement with the expected range of the values for two- and three-ion electrolytes, consistent with their formulae [49].

3.2.4. NMR spectra. The NMR spectra of $L^{1a}H_2$ are very similar to $L^{1b}H_2$. The only difference is the absence of singlets at 2.25 ppm in the ^1H NMR and at 20.7 ppm in the ^{13}C NMR spectra of the latter. In both compounds the signals belonging to the protons of the phenolic hydroxy groups were broad, indicating acidic protons and suggesting formation of O–H–N hydrogen bonds. This has been observed in similar systems [14]. The ^1H NMR spectra of $[ZnL^{2a}Zn(OAc)]PF_6$ have a single resonance at 2.28 ppm, attributed to the six tolyl methyls and indicate that the two methyls are equivalent. ^{13}C NMR spectra of the dizinc macrocyclic complexes show signals for one half of the molecule. These results are consistent with symmetrical structures for $[ZnL^{2a}Zn(OAc)]PF_6$ and $[ZnL^{2b}Zn(OAc)]PF_6$.

3.2.5. Electrochemical properties. Electrochemical properties of copper(II) complexes were studied by cyclic voltammetry in acetonitrile. Typical examples of cyclic voltammograms are provided in "Supplementary material" and the numerical data are provided in table 4. In the sweep to negative potential, complexes containing L^a and L^b demonstrate a reversible or quasi-reversible couple at -0.82 ± 0.03 V and -0.97 ± 0.01 V (*vs.* Ag/Ag^+), respectively, that is attributed to Cu(II)/Cu(I) process in the iminic N_2O_2 coordination site. The reduction potential for complexes with L^b is lower relative to those of L^a due to electron withdrawing of bromine in the phenyl ring that reduces the electron density around copper. Also, $[CuL^{3a}Cu(OAc)]PF_6$ showed

Table 4. Redox potentials and peak separations for copper complexes.

Complexes	$E_{1/2}$[a], V($E_{pa} - E_{pc}$, V)	
	N_2O_2 site Cu(II)/Cu(I) couple	N_2O_2 site Cu(II)/Cu(I) couple
$[(H^+)L^{3a}Cu]PF_6$	−0.82 (0.12)	–
$[(H^+)L^{3b}Cu]PF_6$	−0.96 (0.14)	–
$[ZnL^{2a}Zn(OAc)]PF_6$	−0.83 (0.06)	–
$[ZnL^{2b}Zn(OAc)]PF_6$	−0.98 (0.05)	–
$[ZnL^{3a}Cu(OAc)]PF_6$	−0.85 (0.05)	–
$[ZnL^{3b}Cu(OAc)]PF_6$	−0.98 (0.06)	–
$[CuL^{3a}Cu(OAc)]PF_6$	−0.80 (0.05)	−0.42 (0.09)

[a]1.0 mmol L^{-1} sample, 0.1 mol L^{-1} n-Bu_4NPF_6 in CH_3CN. Scan rate: 100 mVs^{-1}. Solutions were deaerated with Ar for 10 min prior to each run. Condition: Glassy carbon working, Pt auxiliary, Ag/Ag^+ reference electrodes.

another reduction couple at −0.42 V that is attributed to the Cu(II)/Cu(I) reduction in the aminic N_4O_2 compartment. The high Cu(II)/Cu(I) potential in the aminic site compared with that of the iminic site is due to more flexibility of the former to provide a non-planar environment preferred for Cu(I) [30].

3.2.6. X-ray structure. Crystal structure of $[(H^+)L^{3a}Cu]PF_6$. The structure is shown in figure 1 and selected bond lengths and angles are provided in table 5.

The cation comprises $(L^3)^{2-}$ and one Cu(II). The hexafluorophosphate is not coordinated. X-ray crystallography clearly demonstrates that Cu(II) resides in the $N(imine)_2O_2$ site and a proton at the $N(amine)_2O_2$ site, indicating that migration occurred in which Cu(II) shifts from the $N(amine)_2O_2$ site to the $N(imine)_2O_2$ site of $(L^2)^{2-}$ in the cyclization process. During the cyclization one propionitrile pendant is lost. Another propionitrile pendant arm is positioned in the apical site of the basal plane with Cu(1)–N(5) distance 2.897(4) Å, coordinated weakly to copper(II) because of the strong Jahn–Teller effect and can be driven out from the coordination sphere by solvent. The $[CuN(imine)_2O_2]$ chromophore involved in the aromatic moieties is nearly coplanar with deviations from the least-squares plane through CuN_2O_2 of N(1) −0.126, N(2) 0.127, O(1) 0.151, O(2) −0.152 Å, and Cu(II) resides in the plane. The Cu–N and Cu–O bond distances are 1.985(15) and 1.920(7) Å. The N(1)–Cu(1)–N(2) bite angle [96.76(14)°] is significantly larger than 90° and the opposite O(1)–Cu(1)–O(2) angle [80.89(11)°] is smaller than 90°. The cavity at the unfilled site of the ligand has "diagonal" distances of 3.532 Å (O(1)–N(4)) and 4.162 Å (O(2)–N(3)), suitable for a first row divalent transition metal ion, for which M–N and M–O bond distances are generally close to 2 Å. The 1,3-diaminopropane fragment is disordered and located in two positions with a skew conformation. N(1) and N(2) are above and below of the mean macrocyclic plane.

Crystal structure of $[ZnL^{2a}Zn(OAc)]PF_6$. The crystal structure of this compound is shown in figure 2 together with the numbering scheme. Selected bond distances and angles are given in table 6. The compound consists of two monomers in asymmetric units, which are different from a crystallographic point of view. The conformations of the two independent complexes are almost the same, with only differences in bond

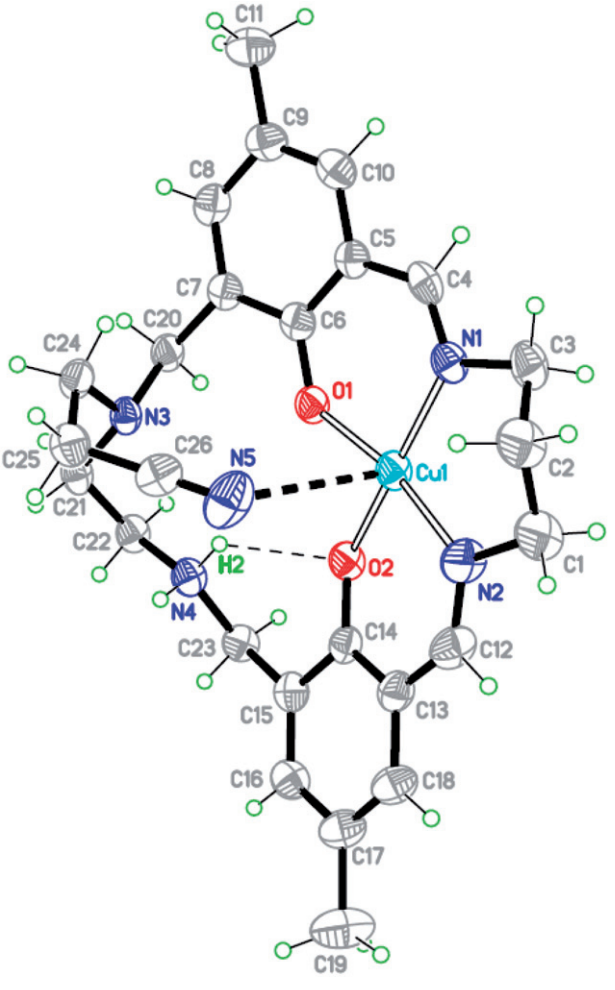

Figure 1. ORTEP diagram of $[(H^+)L^{3a}Cu]PF_6$.

Table 5. Selected bond lengths (Å) and angles (°) for $[(H^+)L^{3a}Cu]PF_6$.

Cu(1)–O(1)	1.913(3)	Cu(1)–N(5)	2.897(4)
Cu(1)–O(2)	1.927(3)	N(5)–C(26)	1.141(5)
Cu(1)–N(1)	1.974(3)	N(3)–C(20)	1.478(5)
Cu(1)–N(2)	2.010(3)	N(4)–C(22)	1.495(5)
N(3)–C(15)	1.461(6)		
O(1)–Cu(1)–O(2)	80.89(11)	O(1)–Cu(1)–N(5)	78.51(11)
O(1)–Cu(1)–N(1)	92.68(12)	O(2)–Cu(1)–N(5)	82.82(12)
O(2)–Cu(1)–N(1)	168.48(12)	N(1)–Cu(1)–N(5)	105.39(13)
O(1)–Cu(1)–N(2)	168.45(13)	N(2)–Cu(1)–N(5)	92.55(14)
O(2)–Cu(1)–N(2)	90.84(13)	N(5)–C(26)–C(25)	179.1(5)
N(1)–Cu(1)–N(2)	96.76(14)		

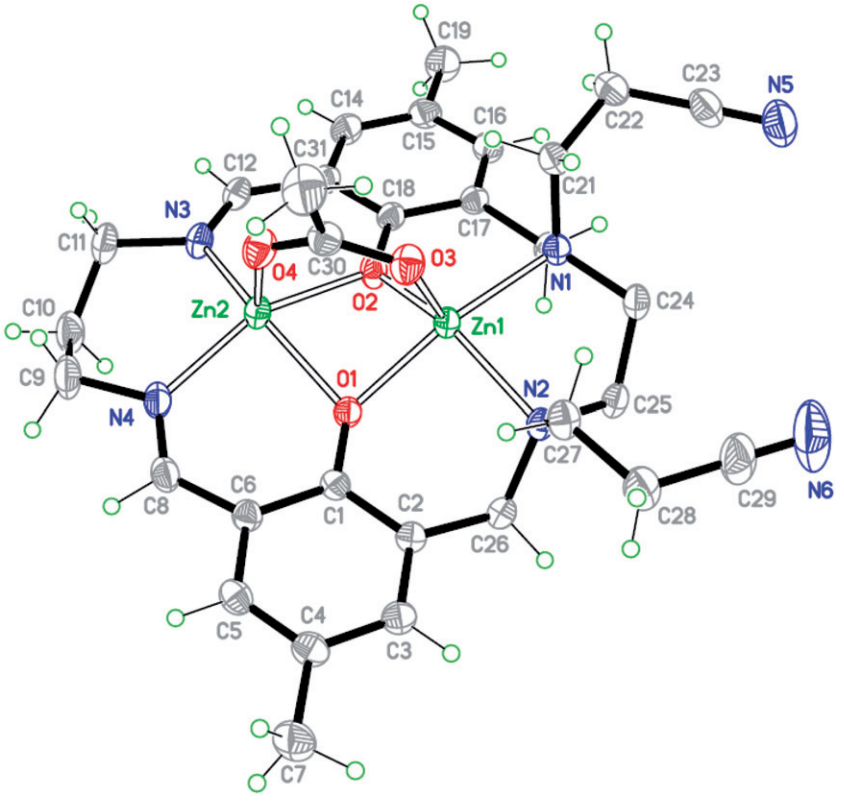

Figure 2. ORTEP diagram of $[ZnL^{2a}Zn(OAc)]PF_6$.

distances and angles. Each cation has $(L^2)^{2-}$, two Zn(II) and one acetate. One Zn(II) resides at the $N(amine)_2O_2$ site and another at the $N(imine)_2O_2$ site. The pair of zinc ions is bridged by two phenolic oxygen atoms and an acetate, providing distorted five-coordination. The Zn–Zn separation is 2.9514(4) Å and 2.9688(4) Å for two asymmetric units. The geometry around Zn(1) bound to the $N(amine)_2O_2$ can be regarded as a square pyramid: the parameter τ [50] discriminating between square pyramid ($\tau = 0$) and trigonal bipyramid ($\tau = 1$) is 0.024. The equatorial Zn(1)–$N(amine)_2O_2$ bond distances fall in the range 2.0079(19)–2.131(2) Å and the axial Zn(1)–O(3) bond is 1.960(2) Å. The deviation of the Zn(1) from the basal $N(amine)_2O_2$ least-square plane toward O(3) is 0.544(4) Å. The $[Zn(2)N(imine)_2O_2]$ site is almost square pyramidal ($\tau = 0.154$) with basal Zn(2)–O and Zn(2)–N bond distances Zn(2)–O(1) = 2.0755(18) Å, Zn(2)–O(2) = 2.0394(19) Å, Zn(2)–N(3) = 2.026(2) Å, and Zn(2)–N(4) = 2.039(3) Å, which are shorter than the corresponding basal Zn(2)–O and Zn(2)–N bond distances. Instead, the apical Zn(2)–O(4) is long (2.011(2) Å). Because of the acetate bridge, the $N(amine)_2O_2$ and the $N(imine)_2O_2$ least-square plane are bent at the O(1)–O(2) edge of 165.87(4)°. The deviation of Zn(2) from the basal $N(imine)_2O_2$ least-squares plane toward O(4) is 0.453 Å. The $[ZnL^{2a}Zn]$ entity assumes a saddle-like shape with a bridging acetate on the saddle. The O(1)–C(1) and the O(2)–C(18) bonds make an angle of 161.89°. The dihedral angle between the least-squares plane defined by Zn(1), O(1),

Table 6. Selected bond lengths (Å) and angles (°) for $[ZnL^{2a}Zn(OAc)]PF_6$.

Zn(1)–O(1)	2.0459(19)	Zn(1′)–O(1′)	2.0578(19)
Zn(1)–O(2)	2.0079(19)	Zn(1′)–O(2′)	2.017(2)
Zn(1)–O(3)	1.960(2)	Zn(1′)–O(3′)	1.959(2)
Zn(1)–N(1)	2.131(2)	Zn(1′)–N(1′)	2.121(2)
Zn(1)–N(2)	2.117(2)	Zn(1′)–N(2′)	2.120(2)
Zn(1)–Zn(2)	2.9514(4)	Zn(1′)–Zn(2′)	2.9688(4)
Zn(2)–O(1)	2.0755(18)	Zn(2′)–O(1′)	2.0831(19)
Zn(2)–O(2)	2.0394(19)	Zn(2′)–O(2′)	2.033(2)
Zn(2)–O(4)	2.011(2)	Zn(2′)–N(4′)	2.035(3)
Zn(2)–N(3)	2.026(2)	Zn(2′)–N(3′)	2.039(3)
Zn(2)–N(4)	2.039(3)	Zn(2′)–N(4′)	2.035(3)
N(3)–C(12)	1.274(4)	N(3′)–C(12′)	1.278(4)
N(4)–C(8)	1.281(4)	N(4′)–C(8′)	1.275(4)
C(23)–N(5)	1.138(5)	C(23′)–N(5′)	1.124(5)
C(29)–N(6)	1.162(9)	C(29′)–N(6′)	1.17(2)
O(3)–Zn(1)–O(2)	106.19(9)	O(3′)–Zn(1′)–O(2′)	106.17(10)
O(3)–Zn(1)–O(1)	101.69(9)	O(3′)–Zn(1′)–O(1′)	100.77(9)
O(2)–Zn(1)–O(1)	75.09(8)	O(2′)–Zn(1′)–O(1′)	75.15(8)
O(3)–Zn(1)–N(2)	105.00(9)	O(3′)–Zn(1′)–N(2′)	104.78(10)
O(2)–Zn(1)–N(2)	148.20(9)	O(2′)–Zn(1′)–N(2′)	148.30(9)
O(1)–Zn(1)–N(2)	92.73(8)	O(1′)–Zn(1′)–N(2′)	92.58(8)
O(3)–Zn(1)–N(1)	106.85(9)	O(3′)–Zn(1′)–N(1′)	108.68(10)
O(2)–Zn(1)–N(1)	89.39(8)	O(2′)–Zn(1′)–N(1′)	89.82(8)
O(1)–Zn(1)–N(1)	150.39(8)	O(1′)–Zn(1′)–N(1′)	149.73(8)
N(2)–Zn(1)–N(1)	87.44(8)	N(2′)–Zn(1′)–N(1′)	86.67(9)
O(4)–Zn(2)–N(3)	112.05(10)	O(4′)–Zn(2′)–N(3′)	114.08(11)
O(4)–Zn(2)–N(4)	99.95(11)	O(4′)–Zn(2′)–N(4′)	98.26(11)
N(3)–Zn(2–N(4)	98.15(10)	N(4′)–Zn(2′)–N(3′)	98.42(11)
O(4)–Zn(2)–O(2)	98.58(9)	O(4′)–Zn(2′)–O(2′)	99.36(10)
N(3)–Zn(2)–O(2)	88.63(9)	O(2′)–Zn(2′)–N(3′)	88.53(9)
N(4)–Zn(2)–O(2)	156.15(10)	O(2′)–Zn(2′)–N(4′)	156.44(10)
O(4)–Zn(2)–O(1)	98.90(9)	O(4′)–Zn(2′)–O(1′)	96.42(9)
N(3)–Zn(2)–O(1)	146.46(9)	N(3′)–Zn(2′)–O(1′)	147.20(9)
N(4)–Zn(2)–O(1)	88.58(9)	N(4′)–Zn(2′)–O(1′)	88.34(9)
O(2)–Zn(2)–O(1)	73.79(8)	O(2′)–Zn(2′)–O(1′)	74.27(8)
N(6)–C(29)–C(28)	179.5(5)	N(6′)–C(29′)–C(28′)	176.5(2)
N(5)–C(23)–C(22)	178.3(5)	N(5′)–C(23′)–C(22′)	179.0(5)
O(3)–C(30)–O(4)	125.8(3)	O(4′)–C(30′)–O(3′)	125.8(3)

and O(2) and the least-squares plane defined by Zn(2), O(1), and O(2) is 49.67°. The bridging O(2) has a planar configuration: the sum of the Zn(1)–O(2)–Zn(2), Zn(1)–O(2)–C(18), and Zn(2)–O(2)–C(18) angles is 358.5°. O(2) has a non-planar configuration with the sum of the Zn(1)–O(1)–Zn(2), Zn(1)–O(1)–C(1), and Zn(2)–O(1)–C(1) angles of 338.7°. The two *N*-propionitrile pendant arms attached to N(1) and N(2) are *cis* with respect to the mean molecular plane and on the same side as the bridging acetate.

Crystal structure of $[ZnL^{2a}Cu(OAc)]PF_6 \cdot CH_3CN$. The structure is presented in figure 3 and selected bond lengths and angles are provided in table 7. This structure is similar to the analogous complex reported by Okawa [51, 52]. The compound is a heterodinuclear macrocyclic complex, a PF_6^- and an acetonitrile trapped in the crystal lattice. The Cu(II) is located in the $N(imine)_2O_2$ and Zn(II) in the $N(amine)_2O_2$ sites. Two phenolic oxygen atoms and an acetate bridge the two metal ions. The geometries around both metal ions are square pyramidal but with different degrees of deviations. The discriminating parameter τ is 0.025 for copper(II) and 0.201 for zinc(II).

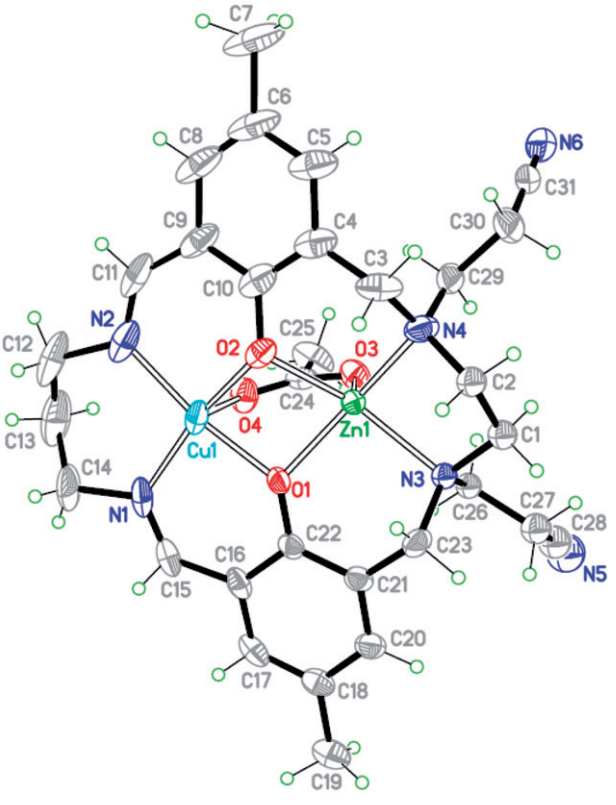

Figure 3. ORTEP diagram of $[ZnL^{2a}Cu(OAc)]PF_6 \cdot CH_3CN$.

Table 7. Selected bond lengths (Å) and angles (°) for $[ZnL^{2a}Cu(OAc)]PF_6 \cdot CH_3CN$.

Zn(1)–O(3)	1.940(3)	Cu(1)–O(2)	1.940(4)
Zn(1)–N(3 A)	2.005(12)	Cu(1)–N(1)	1.973(5)
Zn(1)–O(1)	2.022(3)	Cu(1)–O(1)	1.976(3)
Zn(1)–O(2)	2.061(3)	Cu(1)–N(2)	1.982(5)
Zn(1)–N(4)	2.099(4)	Cu(1)–O(4)	2.260(3)
Zn(1)–N(3)	2.179(6)	Zn(1)–Cu(1)	2.9345(8)
O(3)–Zn(1)–N(3 A)	110.6(4)	O(2)–Zn(1)–N(3)	154.82(18)
O(3)–Zn(1)–O(1)	109.10(14)	N(4)–Zn(1)–N(3)	86.5(2)
N(3 A)–Zn(1)–O(1)	95.3(2)	O(2)–Cu(1)–N(1)	166.42(17)
O(3)–Zn(1)–O(2)	105.22(14)	O(2)–Cu(1)–O(1)	76.77(14)
N(3 A)–Zn(1)–O(2)	144.2(4)	N(1)–Cu(1)–O(1)	91.97(16)
O(1)–Zn(1)–O(2)	73.09(14)	O(2)–Cu(1)–N(2)	91.6(2)
O(3)–Zn(1)–N(4)	107.46(16)	N(1)–Cu(1)–N(2)	99.1(2)
N(3A)–Zn(1)–N(4)	78.1(3)	O(1)–Cu(1)–N(2)	167.9(2)
O(1)–Zn(1)–N(4)	142.79(16)	O(2)–Cu(1)–O(4)	95.73(14)
O(2)–Zn(1)–N(4)	90.96(16)	N(1)–Cu(1)–O(4)	92.01(16)
O(3)–Zn(1)–N(3)	99.42(19)	O(1)–Cu(1)–O(4)	91.08(13)
O(1)–Zn(1)–N(3)	94.12(15)	N(2)–Cu(1)–O(4)	93.36(17)

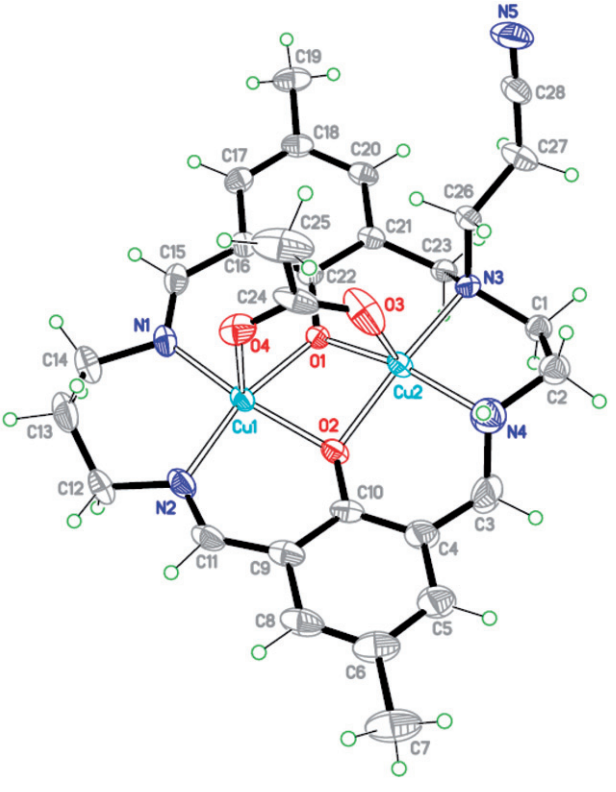

Figure 4. ORTEP diagram of $[CuL^{3a}Cu(OAc)]PF_6 \cdot 1.5\ H_2O$.

The copper(II) is located in the basal plane made by O(1), O(2), N(1), and N(2) and its deviation from the least-squares plane is N(1) −0.029, N(2) 0.029, O(1) 0.036, O(2) −0.036, Cu(1) 0.103 Å. However, the Zn(II) ion is moved toward the acetate bridge, O(3), so that its deviation from the basal $(amine)_2O_2$ (N(3), N(4), O(1), and O(2)) least-squares plane is 0.546 Å. Because of the acetate bridge, $N(amine)_2O_2$ and the $N(imine)_2O_2$ planes are bent at the O(1)–O(2) edge. The angle between the two planes is 157.65(4)°. The two *N*-propionitrile pendant arms attached to N(3) and N(4) are situated *cis* with regard to the mean molecular plane and on the same side of the bridging acetate group.

Crystal structure of $[CuL^{3a}Cu(OAc)]PF_6 \cdot 1.5H_2O$. The crystal structure of this compound is shown in figure 4 together with the numbering scheme. Selected bond distances and angles are given in table 8. The compound consists of a cation dicopper macrocyclic complex, a PF_6^-, 1.5 molecules of water, and an acetate. The cation includes a macrocyclic ligand which has one *N*-propionitrile pendant arm. Both compartments are occupied by Cu(II) with square-pyramidal structures as a result of the presence of a bridging acetate in the apical position of the two copper ions. The copper(II) ions move from basal planes toward oxygen atoms of acetate. The deviation of Cu(1) in the $N(imine)_2O_2$ compartment from the basal plane made by N(1), N(2), O(1), and O(2) is 0.152(10) Å; this deviation for Cu(2) in $N(amine)_2O_2$ coordination site is 0.734(11) Å. The two planes are bent at the O(1)–O(2) edge and the angle between them is 160.66(4)°.

Table 8. Selected bond lengths (Å) and angles (°) for $[CuL^{3a}Cu(OAc)]PF_6 \cdot 1.5\ H_2O$.

Cu(1)–O(2)	1.963(4)	Cu(2)–O(1)	1.953(3)
Cu(1)–O(1)	1.968(3)	Cu(2)–O(2)	1.962(3)
Cu(1)–N(1)	1.969(5)	Cu(2)–N(4A)	1.972(7)
Cu(1)–N(2)	1.979(4)	Cu(2)–N(4)	1.973(7)
Cu(1)–O(4)	2.248(4)	Cu(2)–N(3)	2.012(4)
Cu(1)–Cu(2)	2.9322(8)	Cu(2)–O(3)	2.125(4)
O(2)–Cu(1)–O(1)	76.86(14)	O(1)–Cu(2)–O(2)	77.23(14)
O(2)–Cu(1)–N(1)	166.00(16)	O(1)–Cu(2)–N(4A)	153.9(6)
O(1)–Cu(1)–N(1)	91.46(16)	O(2)–Cu(2)–N(4A)	97.9(2)
O(2)–Cu(1)–N(2)	91.01(18)	O(1)–Cu(2)–N(4)	165.2(3)
O(1)–Cu(1)–N(2	165.34(18)	O(2)–Cu(2)–N(4)	94.4(2)
N(1)–Cu(1)–N(2)	99.3(2)	N(4A)–Cu(2)–N(4)	14.1(4)
O(2)–Cu(1)–O(4)	96.06(16)	O(1)–Cu(2)–N(3)	95.86(16)
O(1)–Cu(1)–O(4)	93.08(14)	O(2)–Cu(2)–N(3)	163.46(17)
N(1)–Cu(1)–O(4)	92.21(17)	N(4A)–Cu(2)–N(3)	81.7(3)
N(2)–Cu(1)–O(4)	96.41(17)	N(4)–Cu(2)–N(3)	88.9(3)
O(2)–Cu(2)–O(3)	96.77(16)	O(1)–Cu(2)–O(3)	98.36(18)
N(4A)–Cu(2)–O(3)	107.7(6)	N(3)–Cu(2)–O(3)	99.12(18)
N(4)–Cu(2)–O(3)	94.7(3)		

The C(1), C(2), and N(4) of the ethylenediamine are disordered and occupy two positions in the crystal structure.

4. Conclusion

The dinucleating macrocyclic ligands containing $N(amine)_2O_2$ and $N(imine)_2O_2$ coordination sites with two propionitrile pendant arms were synthesized by a stepwise method. The synthetic objective of this research was preparation of homo- and heterodinuclear complexes, but in the course of the synthetic studies an unusual bond rupture of one propionitrile pendant arm along with shift of Cu(II) from the $N(amine)_2O_2$ to the $N(imine)_2O_2$ coordination site occurred during cyclization of the acyclic mononuclear copper(II) complexes. To achieve our primary objective, that is the preparation of dicompartmental ligands possessing contiguous six- and four-coordination sites the ligand system requires modification in order to bring the pendant arms in coordination. The –CN moieties of the pendant arms are not able to coordinate to metal ions but it seems possible to transform –CN into $–COO^-$ or $CH_2–NH_2$ groups which contain better donors. Although difficult, the presence of the metal ion could facilitate these transformations. The synthesis of these types of ligands is currently in progress in our lab.

Supplementary material

CCDC 806686, 806685, 822549, and 822548 contain the supplementary crystallographic data for $[(H^+)L^{3a}Cu]PF_6$, $[ZnL^{2a}Zn(OAc)]PF_6$, $[ZnL^{2a}Cu(OAc)]PF_6 \cdot CH_3CN$, and $[CuL^{3a}Cu(OAc)]PF_6 \cdot 1.5H_2O$. These data can be obtained free of charge *via*

www.ccdc.cam.ac.uk/conts/retrieving.html or from the Cambridge Crystallographic Data Centre, 12 Union Road, Cambridge CB2 1EZ, UK; Fax: +44 1223 3366033 or E-mail: deposit@ccdc.cam.uk.

Acknowledgments

We are grateful to Mazandaran University of the Islamic Republic of Iran for the financial support. We also express our appreciation to Dr Sahar Rashid Nadimi for measuring the cyclic voltammogram of the samples.

References

[1] P.A. Vigato, S. Tamburini, L. Bertolo. *Coord. Chem. Rev.*, **251**, 1311 (2007).
[2] P. Guerriero, S. Tamburini, P.A. Vigato. *Coord. Chem. Rev.*, **139**, 17 (1995).
[3] P. Akilan, M. Thirumavalavan, M. Kandaswamy. *Polyhedron*, **22**, 3483 (2003).
[4] S.-Â. Duclos, H. Stoeckli-Evans, T.R. Ward. *Helv. Chim. Acta*, **84**, 3148 (2001).
[5] P.A. Vigato, S. Tamburini. *Coord. Chem. Rev.*, **248**, 1717 (2004).
[6] G.T. Babcock, L.E. Vickery, G. Palmer. *J. Biol. Chem.*, **253**, 2400 (1978).
[7] R.T. Stibrany, R. Fikar, M. Brader, M.N. Potenza, J.A. Potenza, H.J. Schugar. *Inorg. Chem.*, **41**, 5203 (2002).
[8] H. Golchoubian, A. Nemati Kharat. *Polish J. Chem.*, **79**, 825 (2005).
[9] H. Okawa, J. Nishio, M. Ohba, M. Tadokoro, N. Matsumoto, M. Koikawa, S. Kida, D.E. Fenton. *Inorg. Chem.*, **32**, 2949 (1993).
[10] D.G. McCollum, C. Fraser, R. Ostrander, A.L. Rheingold, B. Bosnich. *Inorg. Chem.*, **33**, 2383 (1994).
[11] D.G. McCollum, L. Hall, C. White, R. Ostrander, A.L. Rheingold, J. Whelan, B. Bosnich. *Inorg. Chem.*, **33**, 924 (1994).
[12] C. Fraser, R. Ostrander, A.L. Rheingold, C. White, B. Bosnich. *Inorg. Chem.*, **33**, 324 (1994).
[13] C. Fraser, L. Johnston, A.L. Rheingold, B.S. Haggerty, G.K. Williams, L. Whelan, B. Bosnich. *Inorg. Chem.*, **31**, 1835 (1992).
[14] H. Golchoubian, W.L. Waltz. *Synth. Commun.*, **28**, 3907 (1998).
[15] H. Okawa, H. Furutachi, D.E. Fenton. *Coord. Chem. Rev.*, **174**, 51 (1998).
[16] J. Qian, W. Gu, H. Liu, F. Gao, L. Feng, S. Yan, D. Liao, P. Cheng. *J. Chem. Soc., Dalton Trans.*, 1060 (2007).
[17] K. Matsumoto, K. Sekine, K. Arimura, M. Ohaba, H. Sakiyama, H. Okawa. *Bull. Chem. Soc. Japan*, **77**, 1343 (2004).
[18] T.A. Kaden. *Top. Curr. Chem.*, **121**, 157 (1984).
[19] N.W. Alcock, K.P. Balakrishnan, P. Moore, G.A. Pike. *J. Chem. Soc., Dalton Trans.*, 889 (1987).
[20] K.A. Arnold, L. Echegoyen, F.R. Fronczek, R.D. Gandour, V.J. Gatto, D. White, G.W. Gokel. *J. Am. Chem. Soc.*, **109**, 3716 (1987).
[21] B. Bosnich. *Inorg. Chem.*, **38**, 2554 (1999).
[22] R.W. Hay. In *Current Topics in Macrocyclic Chemistry in Japan*, E. Kimura (Ed.), p. 56, Hiroshima University, Hiroshima (1987).
[23] M. Yonemura, Y. Matsumura, M. Ohba, H. Okawa, D. Fenton. *Chem. Lett.*, 601 (1996).
[24] A. Niazi Rahnama, H. Golchoubian, R. Pritchard. *Bull. Chem. Soc. Japan*, **78**, 1047 (2005).
[25] A. Ghaffarinia, H. Golchoubian, R. Hosseinzadeh. *J. Chin. Chem. Soc.*, **52**, 531 (2005).
[26] H. Golchoubian, E. Baktash, R. Welter. *Inorg. Chem. Commun.*, **10**, 120 (2007).
[27] H. Golchoubian, E. Baktash, R. Welter. *Inorg. Chem. Commun.*, **10**, 1035 (2007).
[28] A. Ghaffarinia, H. Golchoubian. *Polish J. Chem.*, **79**, 83 (2005).
[29] H. Golchoubian, L. Rostami, B. Kariuki. *Polyhedron*, **29**, 1525 (2010).
[30] M. Yonemura, K. Arimura, K. Inoue, N. Usuki, M. Ohba, H. Okawa. *Inorg. Chem.*, **41**, 582 (2002).
[31] H. Furutachi, S. Fujinami, M. Suzuki, H. Okawa. *J. Chem. Soc., Dalton Trans.*, 2761 (2000).
[32] K.-J. Inoue, M. Ohaba, H. Okawa. *Bull. Chem. Soc.*, **75**, 99 (2002).
[33] G.-C. Sun, Z.-H. He, Z.-J. Li, X.-D. Yuan, Z.-J. Yang, G.-X. Wang, L.-F. Wang, C.-R. Liu. *Molecules*, **6**, 1001 (2001).

[34] Bruker Advanced X-ray Solutions. *SMART for WNT/2000 (Version 5.060)*, Bruker AXS Inc., Madison, Wisconsin, USA (1999).
[35] M.C. Burla, R. Caliandro, M. Camalli, B. Carrozzini, G.L. Cascarano, L. De Caro, C. Giacovazzo, G. Polidori, R. Spagna. *J. Appl. Cryst.*, **38**, 381 (2005).
[36] G.M. Sheldrick. *SHELXL-97, Program for X-ray Crystal Structure Refinement*, University of Göttingen, Germany (1997).
[37] *SHELXT LN (Version 5.10)*, Bruker Analytical X-ray Inc., Madison, Wisconsin, USA (1998).
[38] T.F. Bouyagui, G. Mohamed, N.J. Marie, M. Olivier. *J. Chem. Crystallogr.*, **38**, 471 (2008).
[39] M. Yonemura, M. Ohba, K. Takahashi, H. Okawa, D. Fenton. *Inorg. Chim. Acta*, **283**, 72 (1998).
[40] M. Yonemura, Y. Matsumura, H. Furutachi, M. Ohba, H. Okawa, D. Fenton. *Inorg. Chem.*, **36**, 2711 (1997).
[41] R.-G. Xiong, B.-L. Song, J.-L. Zuo, X.-Z. You, X. Huang. *Polyhedron*, **15**, 903 (1995).
[42] H. Okawa, M. Tadakoro, Y. Aratake, M. Ohabo, K. Shindo, M. Mitsumi, M. Koikawa, M. Tomono, D.E. Fenton. *J. Chem Soc., Dalton Trans.*, 253 (1993).
[43] K. Nakamoto. *Infrared and Raman Spectra of Inorganic and Coordination Compounds*, 4th Edn, Section II.8, Wiley-Interscience, New York (1986).
[44] D. Dolphin, A. Wick. *Tabulation of Infrared Spectral Data*, Wiley-Interscience, New York (1977).
[45] J.W. Robinson. *Practical Handbook of Spectroscopy*, CRC Press, Boca Raton, FL (1991).
[46] R.M. Silverstein, G.C. Bassler. *Spectrometric Identification of Organic Compounds*, Wiley & Sons, New York (1998).
[47] J. Lisowski. *Inorg. Chim. Acta*, **285**, 233 (1999).
[48] G.B. Deacon, R.J. Phillips. *Coord. Chem. Rev.*, **33**, 227 (1980).
[49] W.J. Geary. *Coord. Chem. Rev.*, **7**, 107 (1971).
[50] A.W. Addison, T.N. Rao. *J. Chem. Soc., Dalton Trans.*, 1349 (1984).
[51] M. Yonemura, Y. Nakamura, N. Usuki, H. Okawa. *Proc. Indian Acad. Sci.*, **112**, 291 (2000).
[52] J. Costes, F. Dahan, A. Dupuis, J. Laurent. *Inorg. Chem.*, **39**, 169 (2000).